# In Situ Antenna Modeling Tools

V. Cable[1]

*High-fidelity electromagnetic modeling of the performance of low-gain communications antennas on complex spacecraft (including low orbiters, landers, and rovers) has been needed for decades, as evidenced by the requirement for at least a 10-dB margin on all links using low-frequency omni-directional antennas. A difficult area is prediction of performance of low-frequency in situ links. The prediction difficulty stems from the interaction of the antenna with other structures onboard the spacecraft and from the effects of planetary terrain; both of these phenomena can be assessed only by means of detailed computational electromagnetic (CEM) analysis. Experimental methods used in the past are limited and require massive computer hardware. CEM has only recently advanced to the point where accurate prediction of in situ low-gain antenna performance is possible. This article describes an effort that was aimed at establishing such a capability. It describes the progress made toward developing design methods and philosophies that projects can use to minimize the effects of in situ link multipath and onboard electromagnetic interference.*

*Although continual improvement of this CEM capability is intended, the tasks accomplished so far have created a basis that will serve the projects for the next decade, a basis that includes these initial tools, the knowledge to use them, and the validation data indicating their attainable accuracy. It appears that, as a result of this work, the long established 10-dB margin can be significantly reduced, possibly by as much as 6 dB.*

## I. Introduction

JPL has unique requirements for high-fidelity electromagnetic (EM) modeling of the performance of low-gain communications antennas on complex spacecraft, including low orbiters, landers, and rovers for planetary exploration, most notably on Mars and the Moon. The need has existed for decades, as evidenced by the requirement for at least a 10-dB margin on all links using low-frequency omni-directional antennas. In particular, a uniquely difficult area is prediction of performance of low-frequency—ultra-high frequency (UHF) to S-band—in situ links. This prediction is increasingly significant as JPL moves toward routine use of low-frequency, low-gain, omni-directional antennas in such applications. The prediction difficulty stems from the interaction of the antenna with other structures onboard the spacecraft and from the effects of planetary terrain, a major impactor for communication between landed elements of a mission, and both of these phenomena can be assessed only by means of detailed computational

[1] Flight Communications Systems Section.

The research described in this publication was carried out by the Jet Propulsion Laboratory, California Institute of Technology, under a contract with the National Aeronautics and Space Administration.

electromagnetic (CEM) analysis. Although experimental measurements have been used extensively in the past to circumvent the limits of analysis, the experimental methods are often limited and fraught with anomalies caused by the Earthbound measurement setup. Also, until this specific effort was begun, due to the massive computer hardware needed to perform CEM using accepted classical methods to model the full in situ environment, only piecemeal, approximate modeling has been possible. The present 10-dB margin requirement on in situ links is the direct result of the uncertainty in both experimental measurements and piecewise CEM modeling. This 10 dB may very well be an overkill that adds unnecessary costs to projects.

CEM has only recently advanced to the point where accurate prediction of in situ low-gain antenna performance is now possible. However, application of these techniques at JPL has been sporadic, having only been done in response to critical project needs. Instances of such need have increased in frequency with application and concern for low-frequency in situ link communications. The benefits resulting from the initial times that CEM has been applied—Mars Exploration Rover (MER) and Mars Reconnaissance Orbiter (MRO)—have prompted follow-on projects—Phoenix and Mars Science Laboratory (MSL)—to request similar analyses. All this points to a critical need for an established state-of-the-art capability in this area at JPL, and this Interplanetary Network Directorate (IND) effort has been aimed at establishing such a capability, as well as at developing design methods and philosophies that projects can use to minimize the effects of in situ link multipath and onboard electromagnetic interference (EMI).

Antennas are a critical part of every telecommunications link on all JPL missions. The in situ link telecommunications environment includes, but is not limited to, links between landed elements (lander to rover, rover to rover, etc.) and/or between landed elements and overhead elements (orbiter, atmospheric flyer, etc.). Under these conditions, both ends of the link are assumed to be moving relative to one another, and in this environment, the use of low-gain, broad-beam, UHF antennas has the distinct advantage of not requiring steering or pointing. The down side to using a broad field-of-view (FOV) antenna is the increased multipath due to nearby objects (e.g., structures on the rover).

Systems specifications on link margins, e.g., gain, bandwidth, power handling, etc., drive the designs of these link antennas. It is not easy to select the best antenna type and the best location for the antenna to meet these specifications, especially using empirical methods such as mock-up and measurement. These UHF antenna systems are highly coupled to the surrounding media, and the post-launch system link performance is often difficult to ensure. The goal of this development activity is to provide powerful, validated CEM tools to quickly and accurately model the entire antenna–spacecraft in situ environment where FOV, signal-to-noise ratio (SNR), gain, multipath, and near-field EMI all affect the design of high-performance links.

### A. Institutional Impact

Successful completion of this work will enable JPL projects to quickly and accurately design the whole in situ telecommunications environment for maximum link performance between all elements in the in situ mission. Upon completion, these tools will provide accurate predictions of antenna telecommunications performance for all (UHF) in situ spacecraft–lander–rover applications. By using these tools, engineering costs will be reduced because less time (estimation: 1/10) will be required for design and fewer mock-up tests (estimation: 1/10) will be needed for selecting type and placement of in situ antennas. Spacecraft design teams will have accurate predictions of telecommunications link blockage, multipath, and onboard radio frequency (RF) EMI before committing to hardware fabrication or integration. These tools will also provide mission planners with accurate, a priori knowledge of multipath environments they can use to adjust post-launch mission scenarios to maximize the probability of telecommunications link closure.

## II. Objectives

The primary objective of this effort has been to create enhanced antenna analysis and design tools for quickly and accurately assessing in situ link communication performance between landed elements on the surface or between surface and orbital elements. In order to be practical, the goal is to have modeling tools capable of repeated calculations for a computer-aided design (CAD)-based description of the full candidate antenna–spacecraft environment in a reasonable time, e.g., 10 configurations in approximately 8 hours.

Objectives for fiscal year 2004 (FY04) and FY05 can be summarized as follows:

- Demonstrate accuracy and speedup of calculations of multipath and near-fields on large antenna/spacecraft structures.
- Demonstrate multipath and near-field predictions on a spacecraft layout derived directly from a CAD file.
- Demonstrate the new, fast, and accurate FASSTER acoustic research code from the California Institute of Technology (Caltech).
- Demonstrate a 2-D solution of radiation from local sources (antennas) based on Caltech acoustic algorithms.
- Demonstrate the accuracy of multipath predictions for practical spacecraft configurations.

Objectives for FY06 were to demonstrate the accuracy and speedup of calculations of multipath and near-fields on still larger antenna/spacecraft structures.

Each of the above objectives was designed to demonstrate a significant increment of enhancement to JPL's in situ antenna modeling capabilities that has immediate use in JPL project applications.

## III. Approach

### A. Background

JPL currently has many EM analysis and design tools. These simulations are generally done in either of two regimes: (1) low frequencies (LF) where exact, full-wave methods are used or (2) high frequencies (HF) where wavelength is very small compared to the physical dimensions of the body. In the latter case, ray tracing and localized reflection and diffraction mechanisms modeled by physical optics (PO) and/or geometrical optics (GO), geometrical theory of diffraction (GTD), and uniform theory of diffraction (UTD) give good approximations for EM fields. For example, for simple antennas on large bodies (e.g., horn feeding a large reflector), these methods give accurate predictions. On the other hand, these same techniques do not give accurate solutions for antennas located on one or two wavelength bodies (e.g., the MER lander with UHF monopole or MRO with the Electra helix). In order to model wave phenomena associated with these wavelength-sized geometries, the problem must be solved using one of the LF, full-wave techniques.

The LF methods are considered "exact" in the sense that they converge to the exact solution, in the limit, as the number of unknown samples in the problem increases without limit. The LF methods include the finite element (FEM) and finite difference time domain (FDTD) volumetric methods, and the volumetric and surface integral equation (IE) methods. Of all the LF methods, the "gold standard" is generally considered to be the Method of Moments (MoM) surface IE approach [1]. The reason for this is summarized in the following paragraphs.

All LF methods require discretization (sampling) of the geometry. The volumetric differential methods require samples throughout the volume inside and outside the body. Surface integral methods, on the

other hand, need samples only on the surface of the body. The result in either case is a set of $N$ samples where EM boundary conditions are enforced and unknown fields and/or currents are determined. For practical numerical problems, the typical sampling rate in regions where fields and currents vary slowly is approximately 10 mesh points per linear wavelength and 2 to 10 times this rate where fields and currents vary more rapidly (e.g., edges, corners, etc.). In either case (volumetric or surface methods), the numerical problem size grows quickly with physical size (i.e., more wavelengths) and/or with increasing frequency (smaller wavelengths), or both, which can easily overtax the available computational hardware. The volume method produces a very large "sparse" matrix problem, whereas the surface approach produces a more moderate size, but "dense," matrix problem for the same geometric configuration.

### B. Problem Size and Computational Work

The total problem size in terms of computer memory for the volumetric differential methods (e.g., FEM and FDTD) is proportional to $N$, and the computational work (number of floating point operations) is proportional to $N^2$. For the surface integral approach (e.g., MoM), the memory requirement is proportional to $N^2$ and the computational work is proportional to $N^3$. The following examples illustrate recent applications of these two methods.

For the volumetric FEM approach, calculation of pattern and gain of a 14-element array antenna measuring 1 wavelength by 5 wavelengths produced a sparse matrix equation with 187,000 unknowns and took approximately 15 hours to solve. Most notable was that this was for the antenna alone, i.e., no portion of the host platform (spacecraft) was included, and adding the spacecraft to the model would have been completely out of the question.

For the surface IE MoM approach, the pattern and gain calculation for the Electra helix attached to a simple MRO nadir deck produced a dense matrix equation with 15,000 unknowns and took 2 hours. Most notable in this case was that the solution included multipath caused by various components on the Nadir deck. In comparison, the addition of one solar panel would have increased the model size to approximately $N = 21,000$ samples and taken approximately 5 and 1/2 hours to compute on the same machine, but this low-fidelity model would still leave considerable uncertainties in the predicted UHF multipath results. In order to predict the multipath for the whole spacecraft with confidence, a more accurate simulation would require both solar panels, other antennas, the propulsion system enclosure and fuel tanks, the large X-band reflector antenna, and most other main vehicle structures. This higher-fidelity model would now require approximately $N = 60,000$ samples and need approximately 36 GB of memory and approximately 128 hours on the same computer.

### C. Present-Day Methods

For an in situ UHF telecommunications system, performance is determined by the surroundings—that is, it is not just the isolated antenna performance. JPL has the tools (mentioned above) for predicting the in situ antenna environment, but only in small pieces that fit within the computing platform's memory and can be computed in a reasonable time. This piecemeal approach provides some useful information, but it is only part of the picture. Instead, we still rely on empirical means of building and testing a mock-up to capture the whole "highly coupled" in situ environment, and this makes JPL's current requirement of maintaining a 10-dB margin for all these links a daunting objective.

### D. Integral Equation and the Method of Moments

We seek accurate predictions of UHF in situ telecommunications performance for geometry sizes and RF wavelengths where mutual coupling and EM resonances dominate the near-fields. To be accurate, an EM solver must model all the wave physics and nothing can be left out. Only the exact methods, including those mentioned earlier (FEM, FDTD, and the IE approach), can do this. The FEM and FDTD methods are sometimes referred to as "direct" methods since they solve directly for the fields of interest. The IE method, on the other hand, can be called an "indirect" approach since it solves for the amplitude and phase of secondary sources (e.g., induced electric currents) that radiate the fields of interest.

Both approaches are exact, full-wave methods and have other comparative advantages and disadvantages, and they both require the solution of a formidable matrix problem. Taking all these factors into account, the biggest advantage goes to the surface IE approach because the exact "radiation condition" at infinity is already, analytically, part of the method. The volume methods, on the other hand, use a finite volume mesh enclosing the whole geometry, plus some margin of empty space, and this finite mesh must be terminated by special algorithms that only approximate "infinity." Unfortunately, this approximation is problematic when applied "too close" to the geometry of interest, and this leads to significantly larger computational problems than would otherwise be the case.

The surface IE approach requires the MoM to transform the IE into a set of linear simultaneous equations. This combined IE–MoM approach has become the method of choice for most antenna problems, especially those containing other structures besides the antenna itself. Specific details of the MoM technique are presented in Appendix A of this article.

### E. The Newest Fast Integral Equation Methods

The fast methods in CEM have only been studied and implemented within the past 25 years. The speedup and memory savings promised by these highly accurate accelerated methods are derived by reducing the work of solving the full dense matrix problem by using compressed (sparse) matrix forms and fast matrix-vector multiplies. Various implementations have included the fast multipole method (FMM) of Coifman, et al. [2] and the adaptive integral method (AIM) of Bleszynski, et al. [3]. These methods are considerably faster than the classical non-accelerated FEM and MoM algorithms mentioned above. The conventional methods require $O\{N^2\}$ to $O\{N^3\}$ floating point operations ($N$ = the number of sample points) in contrast with $O\{N\log_2(N)\}$ to $O\{N^{3/2}\log_2(N)\}$ operations for the fast schemes. More recently, a high-order accelerated method was introduced by Bruno and Kunyansky at Caltech [4] that has the advantage of higher-order convergence for the same surface IE problems; the FMM and AIM approaches do not exhibit this higher-order convergence property. As a result, the accuracy of Bruno's method does not deteriorate with increasing problem size, using fewer sample points per square wavelength with $O\{N^{6/5}\log_2(N)\}$ to $O\{N^{4/3}\log_2(N)\}$ operations. This new method gives rise to the promise of significant computer speedup, memory savings, and super-algebraic (faster than exponential) convergence in predicting EM radiation and scattering from electrically large antenna/spacecraft geometries. For example, by using Bruno's method, accurate prediction of UHF antenna performance as well as the UHF EMI environment for a complete MRO spacecraft requiring $N = \sim 60,000$ would take less than 1 hour on a single CPU desktop computer. Also, the same predictions at S-band with $N = \sim 600,000$ would still take less than 1 hour on a massively parallel computer like the JPL Dell Cluster. A summary of the Bruno method is given in Appendix B.

### F. Our Approach

The steps taken by this effort to reach the stated objectives are summarized by the following:

- Adapt existing MoM algorithms to an SGI Origin shared-memory parallel computer environment (JPLM_PAT-p1).
- Implement the interface between CAD files and JPLM_PAT and JPLM_PAT-p1 inputs.
- Install and test Caltech's new fast and accurate FASSTER acoustic research code at JPL.
- Implement and test 2-D antenna code JPLM-fast2D for metallic surfaces based on Caltech acoustic algorithms.
- Adapt the MoM algorithm to an SGI Altix-based OMP shared-memory, distributed-memory computer (JPLM_PAT-p2).

- Adapt MoM algorithms to a Linux-based distributed-memory computer (JPLM_PAT-p3).
- Compare JPLM_PAT simulation results to measured data from physical models and computed results from other exact methods.
- Apply CEM tools to JPL projects for the purpose of gaining experience with the new tools and additional support for advanced CEM tools development.

## IV. Progress

### A. FY04 Results

Early applications of CEM (JPL_PAT) to JPL projects, in 2003, included predictions of in situ UHF antenna performance for MRO. Based on these simulations, the MRO Electra helix antenna was repositioned for improved FOV (less multipath). The extent of MRO CEM modeling, however, was limited to only the nadir deck since the available computing hardware had insufficient memory and speed to do more. This IND in situ antenna project was launched in FY04, largely as a result of this experience.

In FY04, the focus was on the improvement and validation of existing CEM models for accurate prediction of gain and multipath of UHF antennas mounted on spacecraft and/or rovers (e.g., the Electra helix antenna on MRO). The achievements in FY04 are summarized in the following paragraphs.

The existing "serial" MoM code (JPLM_PAT) was ported as JPLM_PAT-px to a multiprocessor SGI Origin (IRIX) with 32 CPUs and 20 GB of memory. JPLM_PAT-P was then compiled and benchmarked for speed and accuracy on a single Origin CPU. The benchmark problem was a 36-element patch array antenna that required $N = 7290$ unknowns and 23 minutes of run time on a 2.3-GHz Dell workstation. The accuracy of the Origin result was comparable to the workstation (approximately $10^{-6}$ average error); however, the single Origin CPU was considerably slower (300 MHz), and the total run time for JPLM_PAT-px was approximately 70 minutes.

Following the above, a parallel matrix equation solver was substituted for the original serial solver. The parallel solver was obtained from the Department of Energy Oak Ridge National Laboratory's Netlib site and installed on the Origin. After modification, the MoM code was renamed JPLM_PAT-p1, and the code was again benchmarked for solution speed and accuracy using 1 CPU. The accuracy was again comparable, the fill time was approximately 64 minutes, and the solve time was approximately 159 minutes. The number of CPUs was then increased (up to approximately 28), and Fig. 1 shows the total run times achieved with an increasing number of active CPUs. In this case, the problem size was $N = 11,646$ unknowns (3600-element patch array).

Ideally, the speedup should scale as the number of CPUs; however, since the matrix fill calculations remain "serial," only $2.1X$ speedup was achieved in going to 4 CPUs and $1.4X$ more in going to 16 CPUs, i.e., calculations for this small problem size are still dominated by the fill time.

The performance of JPLM_PAT-p1 for larger problem sizes (up to $N = 44,046$ unknowns) is illustrated in Fig. 2 for two cases: 1 CPU and 28 CPUs. In this case, since the fill is still done serially, ideally the matrix fill time scales with $N^2$, or $16X$, where $X$ is time for 1 CPU. The solve, however, uses the extra CPUs, so it should scale as $N^3/M$, or $1.7X$ if $M = 28$ is the number of CPUs. The actual fill time for $N = 44,046$ was 13.7 hours ($12.8X$), and the solve time was 5.6 hours ($2.1X$). So, the bottom line result was 19 hours overall with 28 CPUs on the Origin versus approximately 144 hours for a single CPU. The overall run time could be decreased significantly for this size of problem by parallelizing the fill algorithm, and since fill times can be significant even for large problems, parallelization of the fill would be desirable.

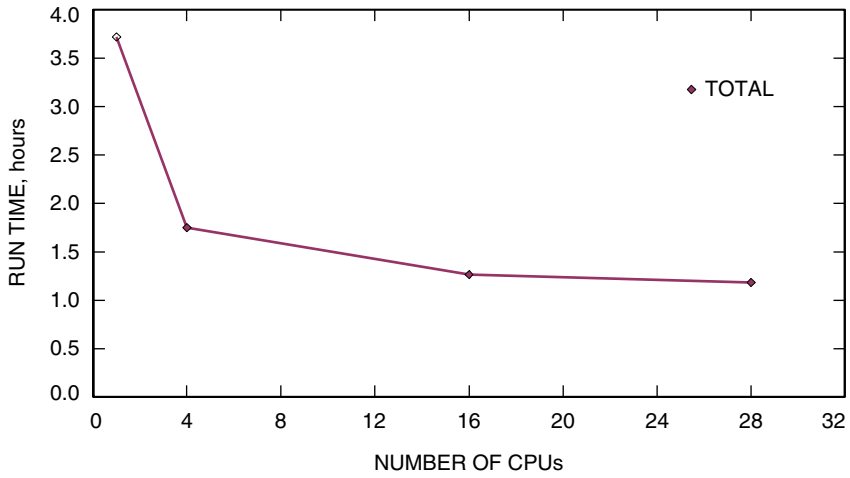


**Fig. 1. Total run time versus number of CPUs (fill and solve for $N$ = 11,646).**

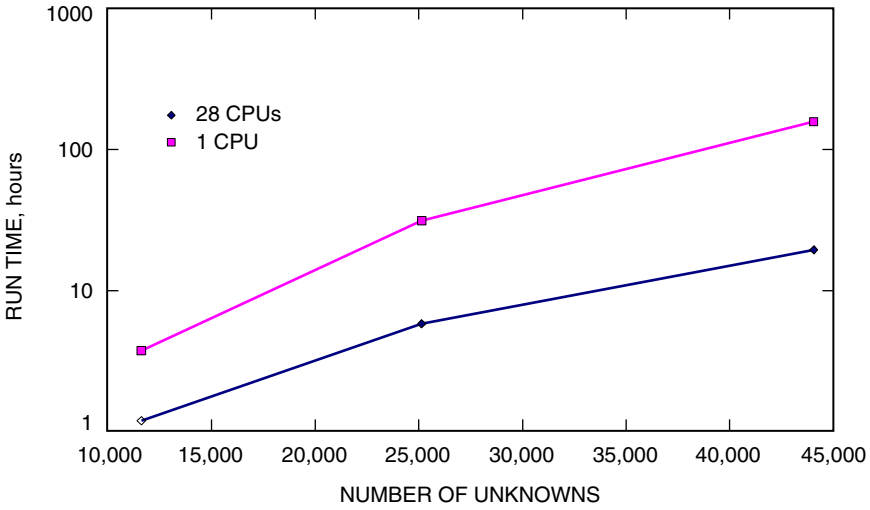


**Fig. 2. Total run time versus problem size (fill and solve ).**

Comparisons of the predicted multipath to available measured data were also accomplished. Predictions of far-field directivity (impedance-matched gain) for a typical in situ link configuration, the MER UHF link configuration, were made since data were available from mock-up measurements made in 2003. The mock-up consisted of the rover deck with panoramic camera (Pancam), high-gain and low-gain X-band antennas, and the UHF link monopole. Figure 3 shows the actual mock-up as mounted for the UHF antenna pattern measurements.

The JPLM_PAT calulations were based on the mesh model shown in Fig. 4. In this case, the number of mesh elements (triangular facets) per linear wavelength is approximately 15 (1 wavelength = 75 cm), producing an $N = 5426$ unknown MoM problem. The measured and computed patterns are compared in Fig. 5, where the x and y coordinates are in the deck plane, $\theta = 0$ deg is the +z (overhead) direction, and $\phi = 0$ deg is the +x (forward) direction. These initial results show very good agreement.

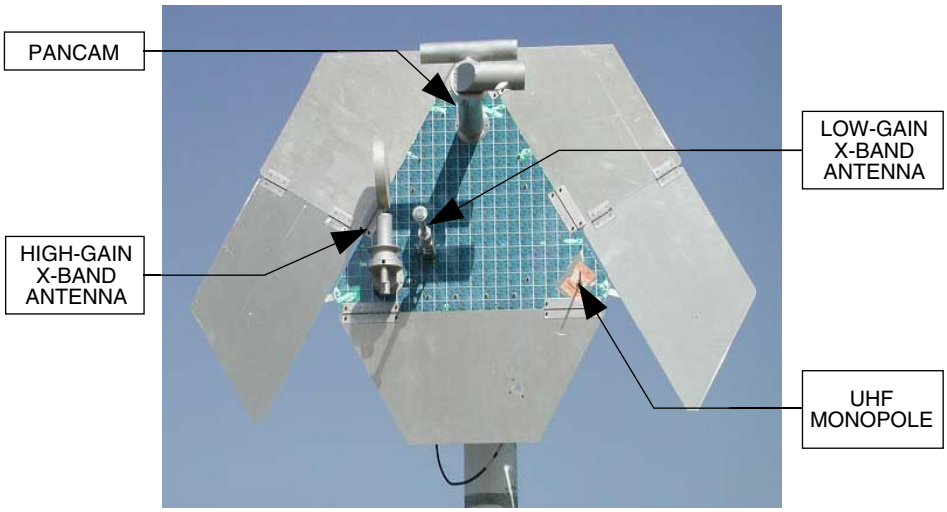


**Fig. 3. MER mock-up for UHF testing.**

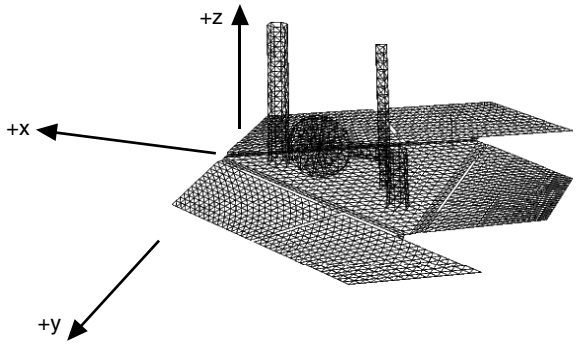


**Fig. 4. MER deck MoM mesh (3290 structured-mesh facets).**

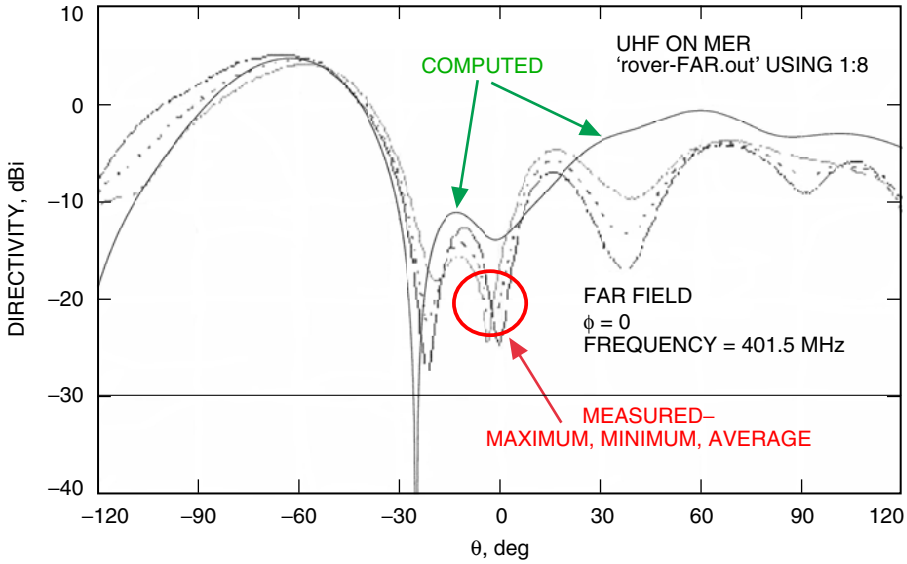


**Fig. 5. MER deck computed versus measured far field ($\phi$ = 90 deg).**

Near-field calculations were also carried out as part of the MRO instrument repositioning study. The MRO nadir deck, shown in Fig. 6 (CAD model and mesh model), was modeled using the near-field option of JPLM_PAT. Figure 7 shows computed near-field electric field intensity ($V/m$) at a plane approximately 30 cm above the nadir deck. Based on these results, the MARCI instrument was eventually relocated to a new nadir deck position, one with a more acceptable level of EMI.

### B. FY05 Results

One of the major achievements in FY05 was the parallelization of the fill algorithm. Figures 8 and 9 show the results obtained for the updated version of JPLM_PAT-p1 running on the same SGI Origin.

Another key accomplishment in FY05 was the establishment of a procedure and an interface in going from engineering CAD drawings of spacecraft to our multipath and near-field prediction software (JPLM_PAT). Until now, all geometry input to JPLM_PAT has been done manually by building a structure from canonical objects (e.g., plates, cylinders, cones, spheres, etc.), the surfaces of which are easily converted to simple, contiguous, "structured," meshes of triangular facets. The geometry figures shown earlier in Figs. 4 and 6 are examples of the structured mesh approach. The facet size in a structured mesh is essentially the same (fixed) throughout. The drawback to the structured approach is the compromise between resolution of key features, like edges and corners where EM fields (and induced electric surface currents) vary rapidly spatially, and the larger central areas without detailed features, where fields and currents vary more slowly. Although a more accurate solution is obtained by sampling more densely (e.g., 200 to 300 facets per square wavelength) in detailed regions, the higher sampling rate generates a larger problem (more unknowns) since structured meshes are normally a fixed facet size. The areas with less detail (e.g., requiring 80 to 100 facets per square wavelength) have far more samples than is necessary in this case. Unfortunately, it is not possible to use a variable-density (block) structured mesh that is also a valid EM mesh.

Construction of a detailed, accurate spacecraft model using the above structured mesh approach is essentially impossible. Also, since the MoM prediction engine is "exact," for a given input geometry, the

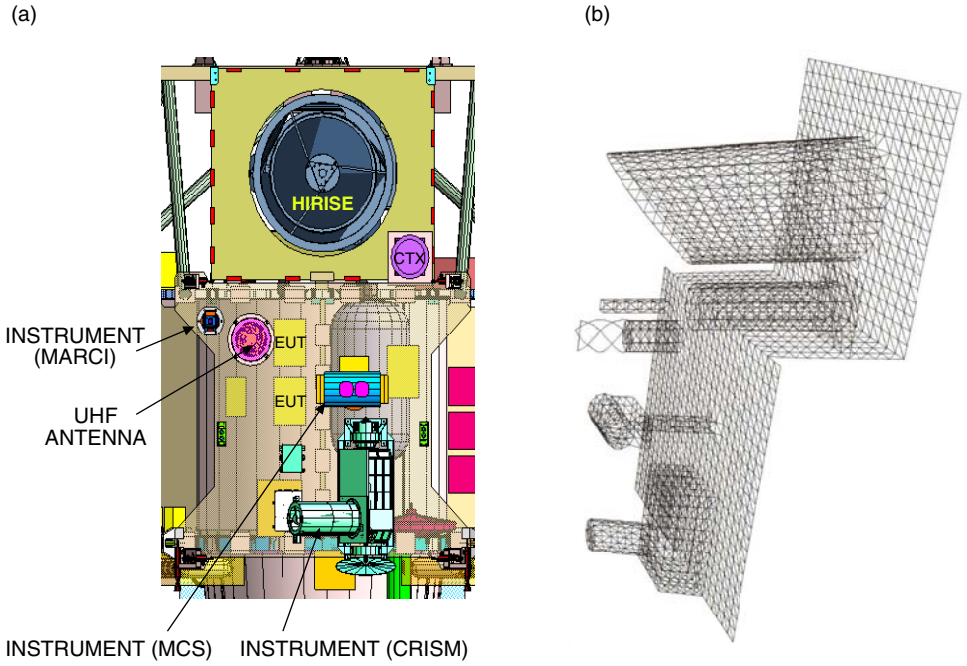


**Fig. 6. The MRO nadir deck: (a) CAD model top view of the layout and (b) JPLM_PAT mesh model oblique view.**

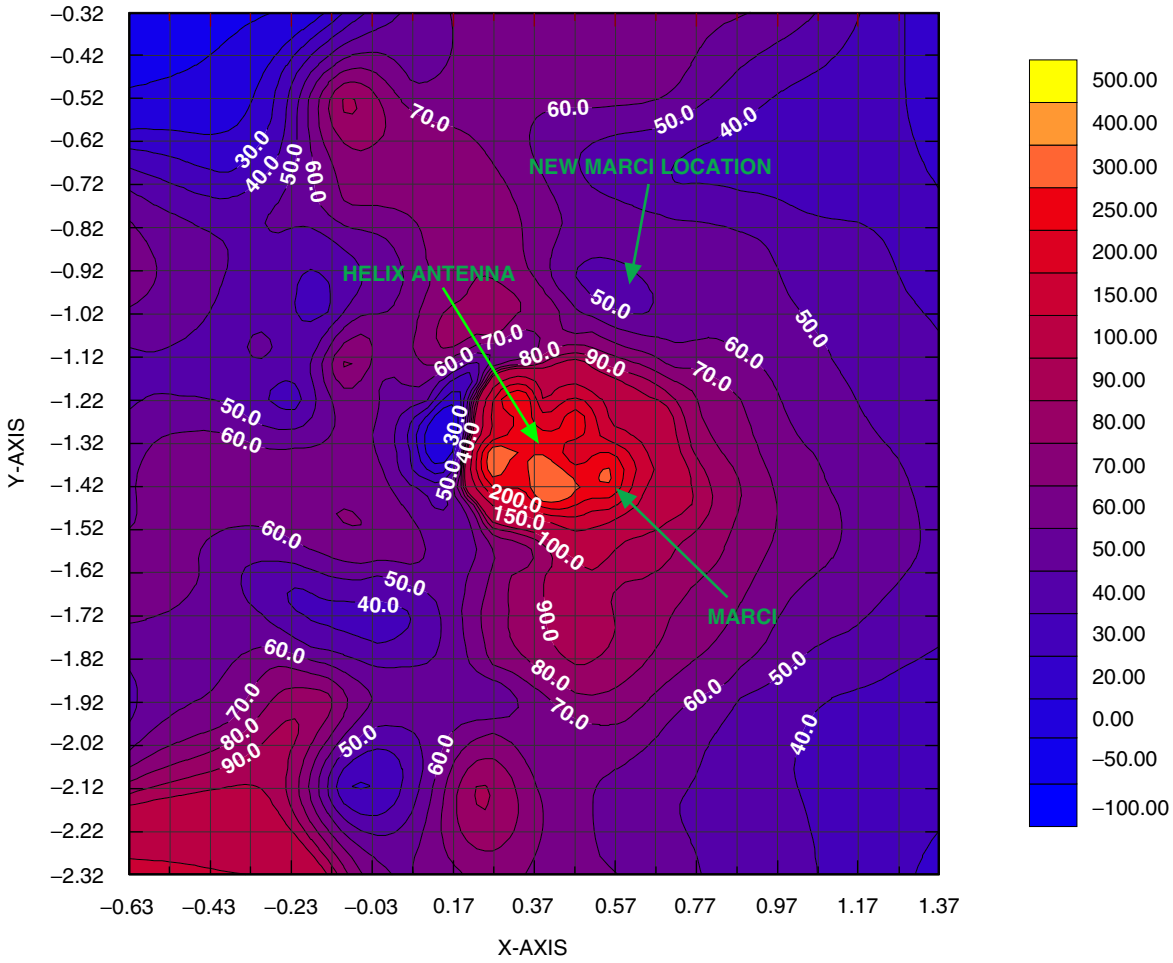


**Fig. 7. Computed near-field electric field intensity at a plane approximately 30 cm above the nadir deck (**near-field $z$ = 1.49**).**

predictions of multipath and/or near-fields for such a model are approximate, at best. To be representative of the true antenna–spacecraft configuration, the MoM calculations must be based on the actual engineering CAD model.

Our solution to this problem is two-fold. First, the data in the full-model CAD file(s) must be filtered only to exterior surfaces that will interact with the EM waves. This function involves manipulations within the CAD software (e.g., Unigraphics). Once the appropriate "exterior" surfaces are defined and written out in an appropriate format, a CAD-to-JPLM_PAT interface converts surface data to contiguous triangle-faceted surfaces with smoothly variable facet densities selected by the user. This latter property is the essence of an "unstructured" mesh.

In order to implement the required IGES-to-unstructured mesh capability, a commercial software package (GID) was purchased and installed on a JPL workstation. An example of a mesh that results from this process is the MER deck with Pancam support and high-gain antenna (HGA), only this time the mesh density is varied to provide improved EM fidelity (Fig. 10).

In Fig. 11, far-field hemispherical pattern results from JPLM_PAT calculations for the UHF monopole using this new mesh model are compared with measurements from mock-up. Although some differences are apparent in the geometry, e.g., Pancam is missing from the calculation, agreement is considered good for the major pattern characteristics.

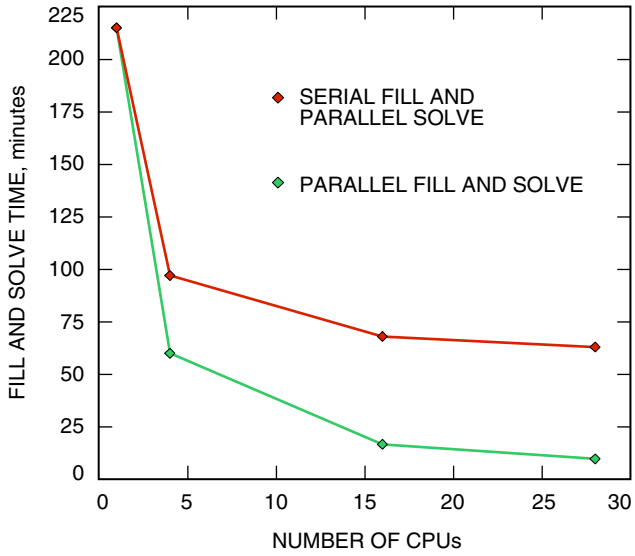


**Fig. 8. Fill and solve time versus number of CPUs (*N* = 11,646).**

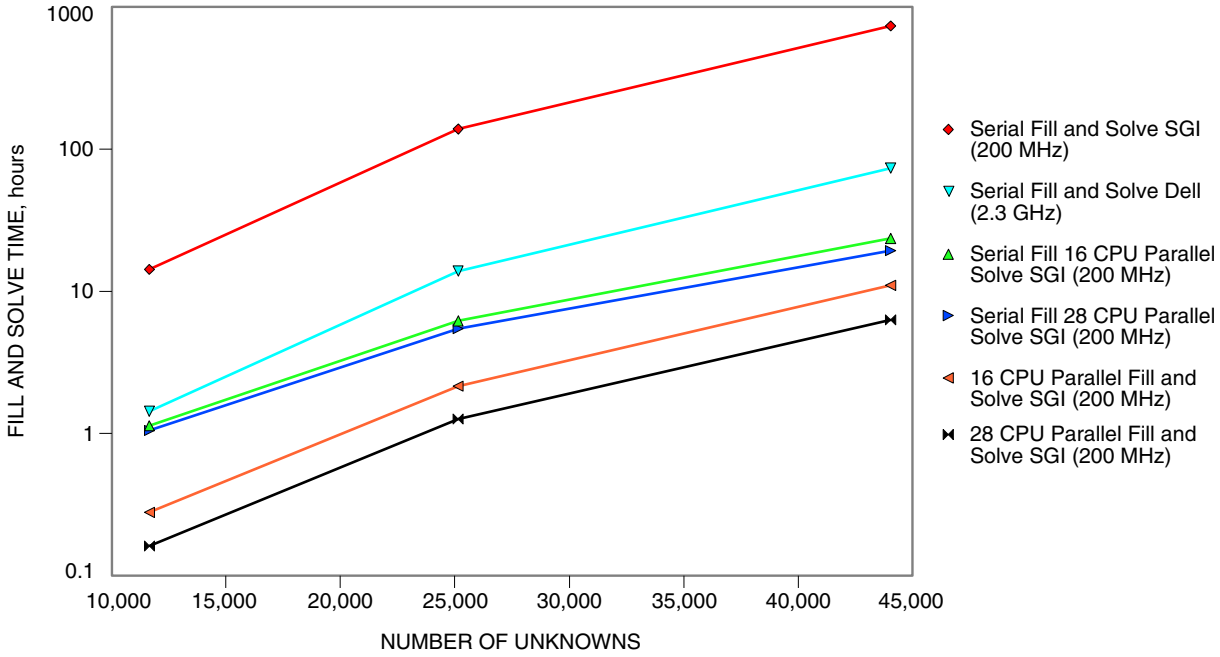


**Fig. 9. Summary of fill and solve time versus number of unknowns.**

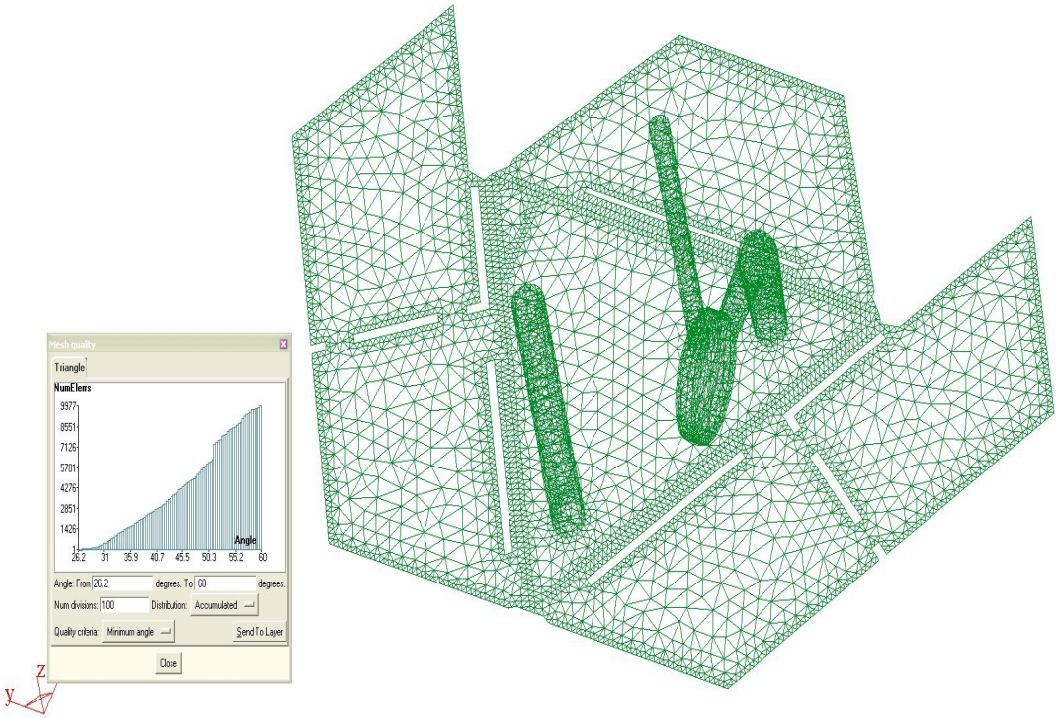


**Fig. 10. Unstructured mesh of MER for MoM calculations (using a commercial software package, GID).**

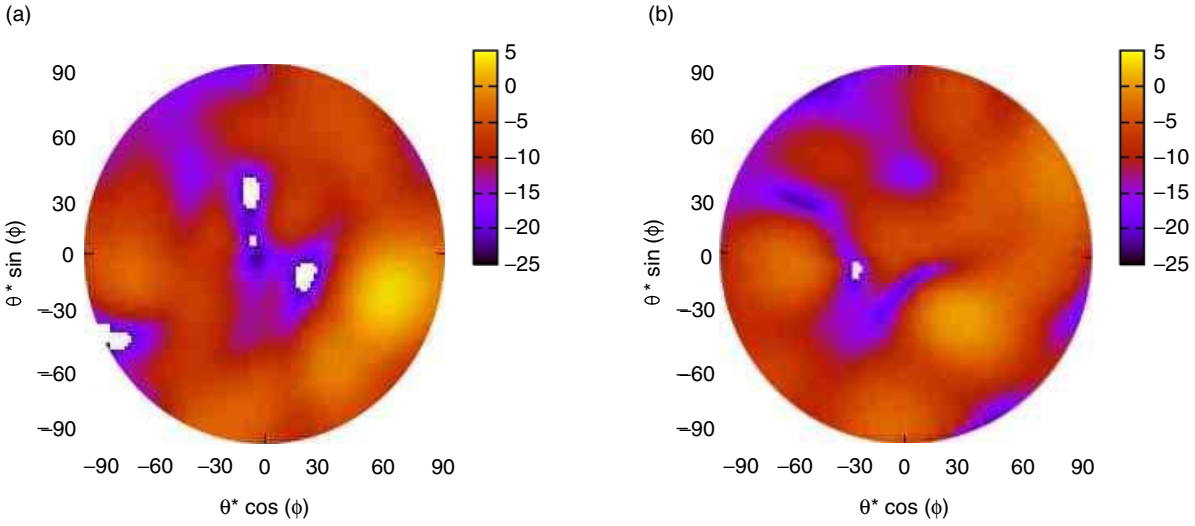


**Fig. 11. Far-field hemispherical pattern results from JPLM_PAT calculations for the UHF monopole using the new mesh model (zenith to 90 deg): (a) mock-up measured pattern and (b) calculated pattern.**

## V. Summary of Project Status

Near-term tasks for FY04–FY05 were completed, and most recent FY06 development of the unstructured mesh capability for the MoM CEM engine was very successful. The last near-term task of benchmarking the speed and accuracy for a large, unstructured, mesh problem requiring a large multiprocessor supercomputer was not completed due to loss of funding for the effort.

The long-term FY07–FY08 roadmap is as follows:

- Implement a 3-D vector version of JPLM_PAT-P2 in the new JPLM_PAT-P3 code.
- Compare the new 3-D Maxwell results to measured data from previously built physical models and to computed results from
  - FDTD-based simulation
  - FEM-based simulation
- Implement the latest Caltech developments in
  - Surface descriptions
    - Interface to CAD models
    - Surface parameterization
  - Wire models (lossless and lossy)
    - Thin
    - Fat
    - Source terminals
    - Lumped loading
  - Thin surface models (lossless and lossy)
    - Closed surfaces
    - Open surfaces
  - Dielectric models (lossless and lossy)
    - Volumetric
    - Thin slab
    - Multimaterial interface
  - Surface singularities
    - Edges
    - Corners
  - Integral equations
    - Electric field integral equation (EFIE)
    - Magnetic field integral equation (MFIE)
    - Combined field integral equation CFIE)
  - Acceleration methods

        - Fast Fourier transform (FFT)-based

- Hybridize the latest Caltech developments with new high-frequency methods
- Incorporate the above results into a validated suite of in situ antenna modeling tools for 3-D EM analysis and design and rules for choosing the best method(s) for the problem at hand:
    - Integral equation
        - EFIE
        - MFIE
        - CFIE
    - Basis functions
        - Rao–Wilton–Glisson (RWG)
        - Nystrom
        - Partitions of unity
    - FFT accelerator
        - Parallel planes
        - Skew planes
    - Method of auxiliary sources (MAS)
    - FMM

Potential customers include all the Mars and lunar programs and deep-space programs using lower-frequency in situ antennas requiring communication with other spacecraft, landers, or outposts.

## References


[1] R. Harrington, *Field Computation by Moment Methods*, Krieger Publishing Co., reprint, 1982.

[2] R. Coifman, V. Rokhlin, and S. Wandzura, "The Fast Multipole Method for the Wave Equation: A Pedestrian Prescription," *IEEE Antennas and Propagation Magazine*, vol. 35, no. 3, pp. 7–12, June 1993.

[3] E. Bleszynski, M. Bleszynski, and T. Jaroszewicz, "AIM: Adaptive Integral Method for Solving Large-Scale Electromagnetic Scattering and Radiation Problems," *Radio Science*, vol. 31, no. 5, pp. 1225-1252, 1996.

[4] O. P. Bruno and L. A. Kunyansky, "Surface Scattering in Three Dimension: An Accelerated High-Order Solver," *Proc. of Royal Society of London A*, vol. 457, pp. 2921–2934, 2001.

[5] S. M. Rao, D. R. Wilton, and A. W. Glisson, "Electromagnetic Scattering by Surfaces of Arbitrary Shape," *IEEE Transaction on Antennas and Propagation*, vol. AP-30, no. 3, pp. 409–418, May 1982.

[6] J. R. Phillips and J. K. White, "A Precorrected-FFT Method for Electrostatic Analysis of Complicated 3-D Structures," *IEEE Trans. on Computer-Aided Design*, vol. 16, no. 10, pp. 1059–1072, October 1997.

# Appendix A
# Details of the Method of Moments Approach

The JPLM_PAT code is an implementation of the IE–MoM method for good electrical conductors. In this case, the IE is the electric field type (EFIE) and is derived by assuming the total electric field $\mathbf{E^{total}} = \mathbf{E^i} + \mathbf{E^s}$ inside and outside $S$, where $\mathbf{E^s}$ can be written as the surface integral of the unknown surface current distribution $\mathbf{J}_s$ times the free-space Green's function on $S$, i.e.,

$$\int_S \mathbf{J_s}(\mathbf{r}')G(\mathbf{r}-\mathbf{r}')ds = \mathbf{E^s}(\mathbf{r})$$

where $G(\mathbf{r}-\mathbf{r}')$ is the free-space Green's function given by

$$G(\mathbf{r}-\mathbf{r}') = \frac{e^{jk|\mathbf{r}-\mathbf{r}'|}}{4\pi|\mathbf{r}-\mathbf{r}'|}$$

and $\mathbf{r}$ and $\mathbf{r}'$ locate the field points and source points, respectively. Finally, the necessary boundary condition on the total electric field on the surface of a perfect electrical conductor $\mathbf{n} \times \mathbf{E^{total}} = 0$ is enforced on $S$ to give the desired EFIE,

$$\int_S \mathbf{J_s}(\mathbf{r}')G(\mathbf{r}-\mathbf{r}')ds = \mathbf{n} \times \mathbf{E^i}(\mathbf{r})$$

The MoM can now be used to convert the above continuous EFIE into the desired matrix equation. The RWG form of MoM is implemented in JPLM_PAT. Once the matrix equation is formed, JPLM_PAT uses a familiar linear algebra technique to solve the system, e.g., the factorization method or conjugate gradient iterative method.

Before applying RWG–MoM, the surface $S$ must be converted (or meshed) into an entire domain of contiguous triangular facets. The two basic constraints on this mesh are that the triangular facets must be as close to equilateral as possible and that no triangular facet should have an edge length greater that 1/10 wavelength. To do otherwise only increases solution error and sometimes also causes numerical singularities that abort the matrix solver.

Once the triangular mesh is generated, all pairs of adjacent facets are said to form a set of overlapping subdomains. Each of these subdomains is assumed to support a sample of the true unknown surface current distribution at that location. We still do not know the true value of these subdomain currents, but since the subdomains are electrically small, we can safely assign unity amplitude current density functions (basis functions) to each subdomain. The total unknown current distribution then becomes a sum of uniform subdomain samples, each multiplied by an unknown scalar coefficient, i.e.,

$$\mathbf{J_s}(\mathbf{r}') = \sum_{n=1}^{N} I_n \mathbf{f_n}(\mathbf{r_n}'), \quad n = 1, 2, 3, \cdots, N$$

where $\mathbf{f}_n(\mathbf{r}'_n)$ is the unity amplitude RWG [5] triangular "rooftop" basis function on the $n$th subdomain located at $\mathbf{r}'_n$. The JPLM_PAT code currently uses the same rooftop basis functions for each subdomain current density sample.

Once the unknown current $\mathbf{J}_s$ has been expanded in terms of $N$ basis functions with unknown coefficients $I_n$, the above equation can be substituted back into the EFIE and the surface integration replaced by the sum of $N$ surface integrations over the $N$ subdomains. The result can be written as the matrix equation

$$\mathbf{ZI} = \mathbf{V}$$

where $\mathbf{Z}$ is the full, dense, $N \times N$ mutual coupling (impedance) matrix with elements

$$[\mathbf{Z_{mn}}] = \int_{S_n} \mathbf{f_n}(\mathbf{r}'_n) G(\mathbf{r_m} - \mathbf{r}'_n), \quad m, n = 1, 2, 3, \cdots, N$$

and $S_n$ is the surface of the $n$th pair of adjacent facets. The unknown current vector $\mathbf{I}$ and known source vector $\mathbf{V}$ are given by

$$\mathbf{I} = [I_n], \quad n = 1, 2, 3, \cdots, N$$

and

$$\mathbf{V} = \big[ -\mathbf{n} \times \mathbf{E^i}(\mathbf{r_m}) \big], \quad m = 1, 2, 3, \cdots, N$$

The above "square" matrix equation is usually solved by standard matrix methods like LU factorization or conjugate gradient.

# Appendix B
# Fast Algorithm Approach

The fast algorithms of Bruno, et al., consist of two main elements: (1) a high-order integrator and (2) a high-order accelerator. The high-order integrator involves the use of partitions of unity (POU) to deal with topological characteristics of the scattering surfaces and analytical resolution of kernel singularities. The high-order accelerator is based on an advanced FFT method developed recently [3,6], and Bruno uses equivalent sources located on a subset of a 3-D Cartesian grid that subdivides the physical geometry (antenna and spacecraft) into cubic cells. The algorithm considers ($\sim\sqrt{N}$) blocks of these cubic cells and places equivalent sources on the 6 faces of these large blocks. Three 2-D FFTs are then used to compute fields of the equivalent sources on the 6 faces of all distant blocks containing the body; "distant" implies more than one block away. The accuracy of this approach increases exponentially as the size of the body is increased, with additional benefits of significantly reduced memory requirements and operation counts for the FFTs.

## I. High-Order Integration

The approach taken here is to perform most, if not all, integrations using the trapezoidal rule in a parameterized space. The parameterization usually takes the form $x = t^n$. The result is super-algebraic convergence to high-order accuracy in every case. In order to make this possible, the integrated function (integrand) must be periodic and infinitely differentiable at both end points of the integration interval, i.e., over one period. This infinitely differentiable (piecewise) integrand is obtained by windowing the original integrand with a function of the form

$$w_j = e^{2[e^{(-1/t)}/(t-1)]}, \quad 0 \leq t \geq 1$$

with

$$\sum_{j=1}^{j=K} w_j = 1$$

where $j = 1, K$ defines $K$ overlapping subdomains. Figure B-1 illustrates this subdomain windowing, also called "partitions of unity." The original integrand is multiplied by these piecewise continuous functions, and the simplest possible integrations are carried out using the trapezoidal rule. Summing these results, including the "normalized" overlapping regions, thus achieves the desired high accuracy.

## II. Resolution of Singularities

The integrands for these CEM problems contain the free-space Green's function, namely,

$$G(\mathbf{r} - \mathbf{r}') = \frac{e^{jk|\mathbf{r}-\mathbf{r}'|}}{4\pi|\mathbf{r} - \mathbf{r}'|}$$

which has a singularity at the point $\mathbf{r} = \mathbf{r}'$. However, a simple conversion to polar coordinates in the local region around the singularity makes the singularity integrable and thus avoids the problem entirely.

## III. Acceleration for Distant Interactions

By far the largest number of integral evaluations needed for these full-wave CEM problems is the calculation of "mutual" interaction, or mutual coupling, between distant points on the physical body (in this case, the antenna–spacecraft structure). In order to speed this calculation, the distant regions in each calculation are each meshed locally in a uniform grid, thus turning the integration into a convolution integral and making an FFT the method of choice. The computational work needed to perform distant calculations now becomes $N\log(N)$ instead of $N^2$. Note that for this technique to work properly the original source points at $\mathbf{r}'$ and field points at $\mathbf{r}$ must be locally projected from the true surfaces onto and off of these uniform grids as equivalent sources. This process can be made fast and efficient, and thus we retain the essence of the $N\log(N)$ savings.

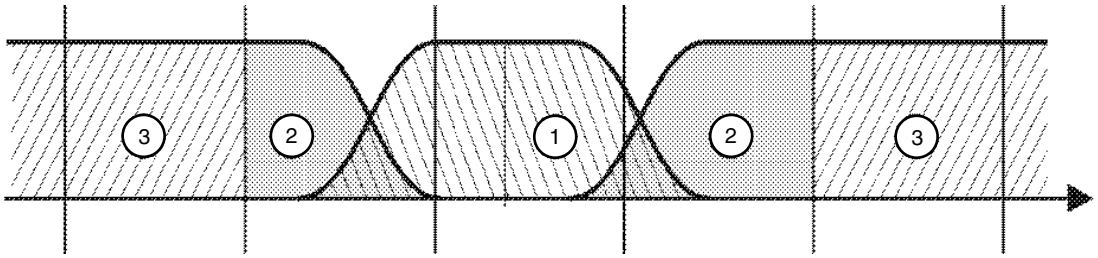


**Fig. B-1. Subdomain windowing.**